

Gate-controlled superconductivity in diffusive multiwalled carbon nanotube

T. Tsuneta¹, L. Lechner^{1,2}, and P. J. Hakonen¹

¹*Low Temperature Laboratory, Helsinki University of Technology, Finland*

²*University of Regensburg, Regensburg, Germany*

(Dated: February 6, 2008)

We have investigated electrical transport in a diffusive multiwalled carbon nanotube contacted using superconducting leads made of Al/Ti sandwich structure. We find proximity-induced superconductivity with measured critical currents up to $I_{cm} = 1.3$ nA, tunable by gate voltage down to 10 pA. The supercurrent branch displays a finite zero bias resistance which varies as $R_0 \propto I_{cm}^{-\alpha}$ with $\alpha = 0.74$. Using IV-characteristics of junctions with phase diffusion, a good agreement is obtained with Josephson coupling energy in the long, diffusive junction model of A.D Zaikin and G.F. Zharkov (Sov. J. Low Temp. Phys. **7**, 184 (1981)).

Superconductivity in carbon nanotubes is an intriguing subject. To understand it one has to consider many facets of modern physics, including Luttinger liquid behavior owing to strong electron-electron interactions in one dimension as well as Kondo physics due to odd, unpaired electronic spin [1]. Intrinsic superconductivity has been observed in ropes of single walled carbon nanotubes (SWNT) [2], while proximity induced superconductivity has been investigated recently in individual SWNTs [3, 4, 5, 6]. The magnitude of the observed supercurrent has varied substantially. In Refs. 3, 4, respectively, a supercurrent on the order of 10x larger and 10x smaller than theoretically expected was observed. Morpurgo *et al.* and Jørgensen *et al.*, on the other hand, did observe only increased conductance near zero bias.

In multiwalled carbon nanotubes (MWNT), supercurrents have been even harder to achieve, presumably due to problems with disorder and impurities. Enhanced conductance was observed by Buitelaar *et al.* [7] near zero bias, which was interpreted in terms of multiple Andreev reflections (MAR) in the presence of inelastic processes [8]. Recently, proximity induced supercurrent has been observed by Kasumov *et al.* [3] as well as by Haruyama and coworkers [9, 10], most notably in multi-shell-contacted tubes grown within nanoporous alumina templates [10]. Here we report proximity-induced superconductivity that is achieved in an individual, diffusive MWNT using bulk(side)-contacted samples with Ti/Al contacts. We find that the supercurrent can be smoothly controlled by gate-voltage, via tuning of the diffusion constant, and a good agreement is obtained using analysis based on long, diffusive SNS junctions supplemented with phase diffusion effects, modeled in terms of the resistively and capacitively shunted junction model (RCSJ).

Our tube material, provided by the group of S. Iijima, was grown using plasma enhanced growth without any metal catalyst [11]. The tubes were dispersed in dichloroethane and, after 15 min of sonication, they were deposited onto thermally oxidized, strongly doped Si wafers. A tube of 4 μm in length and 16.6 nm in diameter was located with respect to alignment markers using a FE-SEM Zeiss Supra 40. Subsequently, Ti contacts of

width 550 nm were made using standard overlay lithography: 10 nm titanium layer in contact with the tube was covered by 70 nm Al in order to facilitate proximity induced superconductivity in Ti at subkelvin temperatures. Last, 5 nm of Ti was deposited to prevent the Al layer from oxidation. The length of the tube section between the contacts was 400 nm. The electrically conducting body of the silicon substrate was employed as a back gate, separated from the sample by 150 nm of SiO₂. An AFM image of our sample is displayed in the inset of Fig. 1.

On our "dipstick" dilution refrigerator (Nanoway PDR50), the samples were mounted inside a tight copper enclosure. The measurement leads were filtered using an RC filter with time constant of 1 μs at 4.2 K, followed by twisted pairs with tight, grounded electrical shields for filtering between still and the mixing chamber, while the final section was provided by a 0.7-m-long Thermocox cable on the sample holder. In the measurements, current bias was employed via a 100 M Ω room-temperature resistor when searching for supercurrents, while voltage bias was employed when looking at multiple Andreev reflections. In the latter case, also the differential resistance $R = dV/dI$ was recorded using lock-in techniques. The gap of the contact material, $\Delta_{lead} = 139$ μeV , was found to be suppressed from our regular gap for Aluminum leads ($\Delta_{reg} = 200$ μeV) by 30 %. Normal state results were measured at $B = 0.2$ T.

Our nanotube sample is slightly n-type doped initially, as in our previous measurements on semiconducting MWNTs [12]. The back gate capacitance $C_g = 4$ aF was deduced from the measured gate period of SET oscillations $\Delta V = 40$ mV. The total capacitance of the 4 μm -long nanotube is estimated to be $C_\Sigma = 0.4$ fF which corresponds to a Coulomb energy of $E_C \sim 2.5$ K. Since the Fermi-level of the tube shifts according to $C_g/C_\Sigma e\Delta V_g$, the number of channels can be varied only in the range of $N \simeq 0$ to a few over the employed gate range of $V_g = -10 \dots + 10$ V. Most of the observed changes in resistance $R(V_g)$ are then due to a variation in the distribution of individual transmission coefficients, not from the changes in N . There is a part of the change,

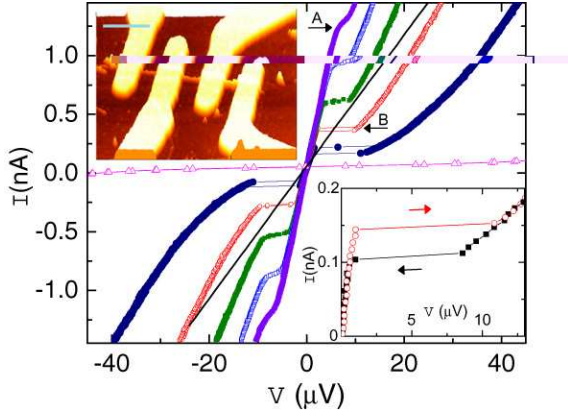


FIG. 1: (color online) Current as a function of bias voltage V at a few values of gate voltage $V_g = 3.214$ V (\bullet); $V_g = 3.220$ V (\circ); $V_g = 3.226$ V (\blacksquare); $V_g = 3.232$ V (\square); $V_g = 3.244$ V (\blacktriangle); $V_g = 3.344$ V (\triangle). The solid straight line displays the normal state IV-curve measured in a magnetic field of $B = 0.2$ T at $V_g = 3.202$ V. The arrows A and B illustrate the determination of the maximum supercurrent I_{cm} in the non-hysteretic and hysteretic cases. The inset on the lower right illustrates a magnification of the low voltage part of the IV-curve at $V_g = 3.214$ V where clear hysteresis is visible and the critical current $I_{cm} = 0.15$ nA. The inset on the upper left displays an AFM image of our sample (scale bar: $1 \mu\text{m}$). The data were measured in a two-lead configuration on the middle section at $T = 65$ mK.

up to 50 % at most (dependent on V_g), that can be attributed to the Kondo effect. Other typical characteristics for our samples are: the mean free path $l_{mfp} \sim 15$ nm and the diffusion constant $D \sim v_F l_{mfp} = 1 \cdot 10^{-2}$ m²/s, as deduced from the resistance. This means that a 400 nm long section (see Fig. 1) is expected to be nearly in the long SNS junction limit. We find several gate voltage values at which the normal state resistance is in the range $R_n = 15 - 20$ k Ω . The regions with good normal state conductance were found to vary by ± 20 mV from day to day. This is attributed to variations in the background charge. Occasionally, we also saw jumps of the background charge which were on the order of 0.1 – 0.3 electrons.

The measured IV-curves are illustrated in Fig. 1. The gate voltage has been varied over 100 mV which corresponds to a change of 2.5 electrons on the island. The shape is seen to change from a state with linear IV-characteristics at small bias to a fully "blockaded" one. The IV-curves in the first category display a pronounced kink, followed by a plateau at voltages in the range of $1 - 10 \mu\text{V}$; at intermediate gate voltages even hysteresis is observed. This behavior is identified as proximity induced superconductivity with the kink/plateau region indicating the maximum measured supercurrent I_{cm} . A more detailed view of the small bias regime is given in the lower right inset of Fig. 1. There is hysteresis at the intermediate values of the critical currents. After a maximum

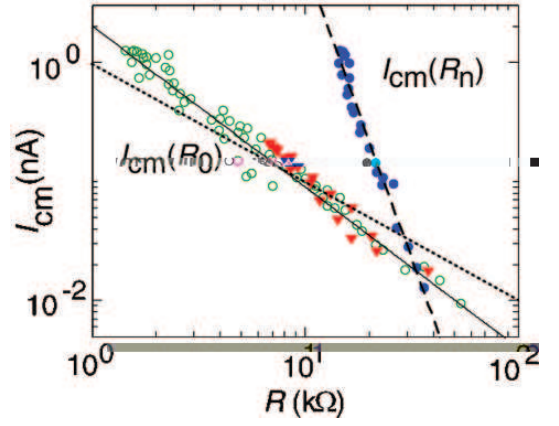


FIG. 2: (color online) Maximum supercurrent I_{cm} vs. zero bias resistance R_0 and normal state resistance R_n measured at $T = 80$ mK. The filled red triangles and the open green circles displays R_0 at gate voltage $V_g = 5.98 \dots 6.02$ V and $3.21 \dots 3.33$ V, respectively. The filled blue circles denote R_n at $V_g = 3.21 \dots 3.33$ V. The solid curve is a power law fit with $I_{cm} \propto R_0^{-1.35}$ while the dashed line represents $I_{cm} \propto R_n^{-4.93}$. The dotted curve displays the phase-diffusion relation $I_{cm} \propto R_0^{-1}$ valid at $E_J \ll k_B T$.

hysteresis of $\Delta I = I_{cm} - I_{retrap} = 54$ pA at $V_g = 3.214$ V, the hysteresis is seen to diminish as the current is lowered. The maximum product for $I_{cm} R_n = 22 \mu\text{eV} \ll \Delta_{lead}$.

According to the RCSJ model, there is hysteresis if the scaled temperature $\Gamma = k_B T / E_J$ is small enough and the McCumber parameter $\beta = (\omega_p R C_{tot})^2 \gg 1$ where ω_p is the plasma frequency, R is the shunt resistance, and C_{tot} is the total capacitance involved in the plasma oscillation. To make an estimate, we take $R = R_J = \frac{dV}{dI} \sim 2$ k Ω from the IV of the junction above the plateau region, $C_{tot} = 400$ fF, and $\omega_p = \sqrt{\frac{2eI_{c0}}{\hbar C_{tot}}}$, we get an estimate $\beta \sim 24$ at $I_{c0} = 5$ nA where $I_{c0} = \frac{2eE_J}{\hbar}$ is taken at $E_J/k_B = 120$ mK. This estimate is close to critical damping and no hysteresis at $\Gamma \sim 1$ is to be expected [13]. Nevertheless, a suppression of $I_{c0} = 5$ nA down to $I_{cm} = 1.3$ nA takes place by thermal fluctuations. When V_g is tuned, R_J increases more strongly than Γ , leading to the appearance of hysteresis in the IV-curves due to a larger value for β . Eventually the increase of Γ with lowering E_J takes over and the hysteresis disappears with decreasing I_{cm} as observed in Fig. 1. Thus, RCSJ model can qualitatively explain the main characteristics observed in Fig. 1.

The supercurrent branch is found to display a finite resistance which depends only weakly on bias (see the inset of Fig. 1). This weakness of bias dependence distinguishes our results from those of Buitelaar et al [7] and of Jørgensen et al [6] who both observed a clear peak in the conductance. The dependence of the measured supercurrent I_{cm} on $R_0 = \frac{dV}{dI}|_{V=0}$ as well as on the normal state resistance R_n is given in Fig. 2. I_{cm} could be

tuned over two orders of magnitude from 1.3 nA down to 10 pA, while the normal state resistance increased only by a factor of two: from 15 to 35 k Ω . We find that the data can be fitted by a power law behavior $I_{cm} \propto R_0^{-1.35}$.

The relatively large zero bias resistance, $R_0 > 1.4$ k Ω , is in agreement with the ordinary picture of phase diffusion [14, 15], which may coexist with hysteretic IV-characteristics provided that the environment of the junction is frequency dependent: at ω_p , $Z_{env} \sim Z_0 = 377$ Ω stabilizing phase diffusion, while at low frequencies $Z_{env} \gg Z_0$ [13]. Ingold *et al.* [16] have derived for the zero bias resistance due to phase diffusion

$$R_0 = \frac{Z_{env}}{I_0(E_J/k_B T)^2 - 1} \quad (1)$$

where $I_0(x)$ represents a modified Bessel function. Subsequently, Grabert *et al.* have shown that Eq. (1) is rather accurate, within a factor of ~ 2 , even when the quantum fluctuations are included [17]. In our analysis, however, we stick to classical phase diffusion because the Coulomb energy E_c in our samples remains small owing to the large, environmental shunting capacitance, which yields $k_B T/E_c \sim 50$ and negligible corrections from the charging effects.

In Ref. 16, the IV-characteristics was derived in the limit $E_J, eV \ll k_B T$, according to which there is a simple relation between I_{c0} and I_{cm} :

$$I_{cm} = \frac{E_J}{4k_B T} I_{c0}. \quad (2)$$

Thus, independent of Z_{env} , one expects $I_{cm} \propto E_J^2$ in the overdamped limit. From the maximum value of $I_{cm} = 1.3$ nA, we get $E_J/k_B = 90$ mK at $T = 65$ mK, which is at the limit of applicability of Eq. (2). Eq. (1) yields $R_0 \propto E_J^{-2}$ in the limit $E_J \ll k_B T$. Therefore, using Eq. (2), we get $I_{cm} \propto R_0^{-1}$, which is seen to coincide quite well with our data in Fig. 2 where this dependence is shown as a dotted line.

The Josephson energy for a long diffusive junction, without interaction effects, can be calculated from the equation [18, 19]

$$I_{C0} = \frac{32}{3 + 2\sqrt{2}} \frac{\epsilon_{Th}}{eR_n} \left(\frac{L}{L_T} \right)^3 \exp\left(-\frac{L}{L_T}\right) \quad (3)$$

which is valid in the limit $\Delta/\epsilon_{Th} \rightarrow \infty$ when $T \simeq 3\epsilon_{Th}/k_B$ and where $L_T = \sqrt{\hbar D/2\pi k_B T}$. We are employing this formula in our analysis as we are not aware of any appropriate theoretical treatment of long, interacting SNS junctions. In SINIS structures, perturbation analysis of the interacting case has shown that there are logarithmic corrections that reduce Josephson coupling [20], but this theory is not suitable for our case as the contacts have a high transparency. We also neglect resonance effects in our analysis, *i.e.* the contribution that might be related to Kondo effect.

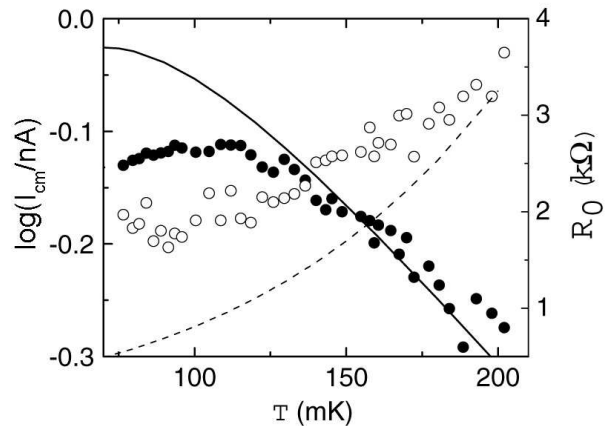


FIG. 3: Temperature dependence of I_{cm} (\bullet) and R_0 (\circ) measured at $V_g = 3.489$ V. The solid curve is a fit obtained from Eqs. (2) and (3) using $D = 2.2 \cdot 10^{-3}$ m²/s, $L = 0.4$ μ m, and $R_n = 17$ k Ω . The dashed line displays R_0 calculated from Eq. (1) using $Z_{env} = 400$ Ω and $E_J(T)$ from the above T -dependence fit.

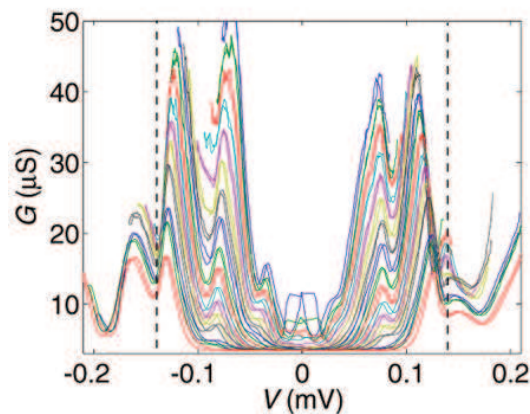


FIG. 4: (color online) Conductance G vs. bias voltage V . Gate voltage V_g has been stepped over $V_g = 3.323 \dots 3.355$ V in steps of 2 mV. The dashed vertical lines indicate locations for the first Andreev reflection process if governed by unrenormalized $\Delta_{lead}/e = 139$ μ eV.

By combining Eqs. (2) and (3), we obtain an analytical formula for I_{cm} that has only one fitting parameter, namely D (or L_T at certain T). In Fig. 3, we compare this formula with the measured temperature dependence of I_{cm} . The solid curve in Fig. 3 is the result of the fit using $L_T = \sqrt{80 \text{ mK}/T}$ 188 nm. This thermal length corresponds to $D = 2.2 \cdot 10^{-3}$ m²/s, yielding $\epsilon_{Th} = 9.0$ μ eV [21]. The discrepancy at the lowest temperatures may be an indication that Eq. (2) becomes invalid and numerical analysis based on the Ivanchenko-Zilberman theory should be done. Deviations at the lowest temperatures are also observed between the fit of Eq. (1) and the measured R_0 in Fig. 3.

Fig. 4 displays the differential conductance G for

the low conductance IV-curves of Fig. 1 in the range $V_g = 3.323 \dots 3.355$ V. A sequence of maxima is seen, which are related to multiple Andreev reflections (MAR) [23, 24]. The MAR peaks are more prominent than what we would expect for a long, diffusive contact on the basis of a recent numerical analysis by Cuevas et al. [22]. The dashed vertical lines indicate locations for the first Andreev reflection process if it is governed by unrenormalized $\Delta_{lead}/e = 139 \mu\text{V}$. Since Coulomb effects tend to shift MAR peaks upwards in voltage, the gap has to be modified at the interface by 20 % downwards, roughly similar to findings by Jørgensen *et al.* [6] in SWNTs with Al/Ti contacts. Using $\tilde{\Delta} = 0.8 \cdot \Delta_{lead} = 111 \mu\text{eV}$ we find that the main Andreev peaks are located at $\frac{2}{3}\tilde{\Delta}$ and $\frac{2}{5}\tilde{\Delta}$, though the latter one does not coincide exactly to the expected location at $V > 0$.

The weak gate dependence of the MAR lines is quite similar to that found in Ref. 7. Between $\tilde{\Delta}$ and $2\tilde{\Delta}$ there is an additional peak that may be connected to Thouless energy. As we approach the supercurrent region by decreasing the gate voltage, ϵ_{Th} (D) increases and, consequently, the peak should move towards $2\tilde{\Delta}$ [22]. In our experiment, however, the peak moves towards $\tilde{\Delta}$. Notice also that in the data of Fig. 4, the supercurrent peak near zero bias starts to develop before any signs of higher order Andreev peaks. This seems to contradict with the scenario of Vecino et al. [8] who argue that inelastic processes enhance conductance due to higher order MAR processes and lead to superconductor-like IV-curves with hysteresis at small bias.

Since the number of transmission channels is rather small in our sample, it is possible that the subgap transport is basically dominated by one single channel. This might result, especially, from the Kondo resonance that is known to play a role in the conductance of good quality MWNTs [7]. In fact, when comparing the shape of the IV curves in Fig. 1 with the calculated IV-curves for single-channel S-N-S contacts [25] rather good agreement is obtained for the range of transmissions $\tau = 0.3 - 0.7$. Therefore, even though a description using the model of a long, diffusive junction seems to work well, presumably an analysis based on a set of transmission channels would yield an even better agreement.

In summary, we have observed proximity-induced superconductivity in a diffusive PECVD-grown MWNT. The Josephson coupling energy could be tuned by gate voltage via a change in the diffusion constant $D \propto 1/R_n$. The model for long diffusive junctions was successfully employed for calculating the dependence of E_J on R_n and T . The measured IV curves (the zero bias resistance R_0 and maximum supercurrent I_{cm}) could be understood using analysis based on classical phase diffusion, which leads to a decrease of I_{cm} as E_J^2 . At $T = 65$ mK, the largest obtained Josephson coupling energy was 0.09 K.

We thank S. Iijima, A. Koshio, and M. Yudasaka for the carbon nanotube material employed in our work.

We wish to acknowledge fruitful discussions with D. Gunnarsson, T. Heikkilä, F. Hekking, P.-E. Lindelöf, M. Paalanen, B. Placais, C. Strunk, and A. Zaikin. This work was supported by the TULE programme of the Academy of Finland and by the EU contract FP6-IST-021285-2.

-
- [1] J. Nygård, D.H. Cobden, and P.E. Lindelof, *Nature* **408**, 342 (2000).
 - [2] A. Yu. Kasumov, R. Deblock, M. Kociak, B. Reulet, H. Bouchiat, I. I. Khodos, Yu. B. Gorbatov, V. T. Volkov, C. Journet, and M. Burghard, *Science* **284**, 1508 (1999).
 - [3] A. Kasumov, M. Kociak, M. Ferrier, R. Deblock, S. Guéron, B. Reulet, I. Khodos, O. Stéphan, and H. Bouchiat, *Phys. Rev. B* **68**, 214 521 (2003).
 - [4] P. Herrero-Jarillo, J. A. van Dam, and L. P. Kouwenhoven, *Nature* **439**, 953 (2006).
 - [5] A. F. Morpurgo, J. Kong, C. M. Marcus, and H. Dai, *Science* **286**, 263 (1999).
 - [6] H. I. Jorgensen, K. Grove-Rasmussen, T. Novotny, K. Flensberg, and P. E. Lindelöf, *Phys. Rev. Lett.* **96**, 207003 (2006).
 - [7] M. R. Buitelaar, W. Belzig, T. Nussbaumer, B. Babic, C. Bruder, and C. Schönenberger, *Phys. Rev. Lett.* **91**, 057 005 (2003).
 - [8] E. Vecino, M. R. Buitelaar, A. Martín-Rodero, C. Schönenberger, and A. L. Yeyati, *Solid State Commun.* **131**, 625 (2004).
 - [9] J. Haruyama, A. Tokita, N. Kobayashi, M. Nomura, S. Miyadai, et al., *Appl. Phys. Lett.* **84**, 4714 (2004).
 - [10] I. Takesue, J. Haruyama, N. Kobayashi, S. Chiashi, S. Maruyama, T. Sugai, and H. Shinohara, *Phys. Rev. Lett.* **96**, 057001 (2006).
 - [11] A. Koshio, M. Yudasaka, and S. Iijima, *Chem. Phys. Lett.* **356**, 595 (2002).
 - [12] F. Wu, T. Tsuneta, R. Tarkiainen, D. Gunnarsson, T. H. Wang, and P. J. Hakonen, *cond-mat/0606661*.
 - [13] J. Martinis and R. Kautz, *Phys. Rev. B* **42**, 9903 (1990).
 - [14] M. Tinkham, *Introduction to superconductivity* (McGraw-Hill, ISBN, 0-07-064878-6, 1996) p. 253.
 - [15] Yu. M. Ivanchenko and L. A. Zil'berman, *Zh. Eksp. Teor. Fiz.* **55** 2395 (1968) (*Sov. Phys. JETP*, **28** 1272 (1969)).
 - [16] G.-L. Ingold, H. Grabert, and U. Eberhardt, *Phys. Rev. B*, **50**, 395 (1994).
 - [17] H. Grabert, G.-L. Ingold, and B. Paul, *Europhys. Lett.* **44**, 360 (1998).
 - [18] A.D. Zaikin and G.F. Zharkov, *Sov. J. Low Temp. Phys.* **7**, 184 (1981). Note that, in the result in this reference, R_n refers to the resistance per one spin channel.
 - [19] P. Dubos, H. Courtois, B. Pannetier, F. Wilhelm, A. Zaikin, and G. Schön, *Phys. Rev. B* **63**, 64502 (2001).
 - [20] C. Bruder, R. Fazio, and G. Schön, *Physica B* **203**, 240 (1994).
 - [21] The values for D and ϵ_{Th} would be 10 - 20 % higher if one would employ a self-consistent numerical evaluation for the product $I_{C0}R_n$. This has been neglected as the main error comes from the lowest order estimate for I_{cm} .
 - [22] J. C. Cuevas, J. Hammer, J. Kopu, J. K. Viljas, and M. Eschrig *Phys. Rev. B* **73**, 184505 (2006).
 - [23] M. Octavio, M. Tinkham, G. E. Blonder, and T. M. Klap-

- wijk, Phys. Rev. B **27**, 6739 (1983).
- [24] K. Flensberg, J. B. Hansen, and M. Octavio, Phys. Rev. B **38**, 8707 (1988).
- [25] D. Averin and A. Bardas, Phys. Rev. Lett. **75**, 1831 (1995); see also, A. Bardas and D. V. Averin, Phys. Rev. B **56**, R8518 (1997).